Published in final edited form as:
Free Radic Biol Med. 2012 June 1; 52(0): 2223–2233. doi:10.1016/j.freeradbiomed.2012.04.003.

Oxidative stress is involved in age-dependent spermatogenic damage of *Immp2l* mutant mice

Sunil K. George, **Yan Jiao**, **Colin E. Bishop**, and **Baisong Lu**[*]
Wake Forest University Health Sciences, Institute for Regenerative Medicine, Winston-Salem, NC 27157

Abstract

Mitochondrial reactive oxygen species (ROS) have been implicated in spermatogenic damage, although direct *in vivo* evidence is lacking. We recently generated a mouse in which the *Inner Mitochondrial Membrane Peptidase 2-like* (*Immp2l*) gene is mutated. This *Immp2l* mutation impairs the processing of signal peptide sequences from mitochondrial cytochrome c1 and glycerol phosphate dehydrogenase 2. The mitochondria from mutant mice generate elevated levels of superoxide ion, which causes age-dependent spermatogenic damage. Here we confirm age-dependent spermatogenic damage in a new cohort of mutants, which started at the age of 10.5 months. Compared with age-matched controls, protein carbonyl content was normal in testes of 2- to 5-month-old mutants, but significantly elevated in testes of 13-month-old mutants, indicating elevated oxidative stress in the testes at the time of impaired spermatogenesis. Testicular expression of superoxide dismutases was not different between control and mutant mice, while that of catalase was increased in young and old mutants. The expression of cytosolic glutathione peroxidase 4 (phospholipid hydroperoxidase) in testes was significantly reduced in 13-month-old mutants, concomitant with impaired spermatogenesis. Apoptosis of all testicular populations was increased in mutant mice with spermatogenic damage. The mitochondrial DNA (mtDNA) mutation rate in germ cells of mutant mice with impaired spermatogenesis was unchanged, excluding a major role of mtDNA mutation in ROS-mediated spermatogenic damage. Our data show that increased mitochondrial ROS are one of the driving forces for spermatogenic impairment.

Keywords

Oxidative stress; *Immp2l*; spermatogenesis; mitochondrial DNA; antioxidant enzyme; mice

Introduction

Mitochondria are membrane-enclosed, multi-functional organelles found in eukaryotic cells. They function as the powerhouse for eukaryotic cells and convert sugar, fat, and protein molecules into ATP via oxidative phosphorylation. Mitochondria also play important roles in apoptosis and intracellular calcium homeostasis [1, 2]. Moreover, they are the primary

[*]To whom all correspondence and proofs should be sent: Baisong Lu, PhD, Wake Forest University Health Sciences, Institute for Regenerative Medicine, Medical Center Boulevard, Winston-Salem, NC 27157, Tel: 336-713-7276, Fax: 336-713-7290, blu@wakehealth.edu.

source of superoxide ions, which can be transformed into other forms of reactive oxygen species (ROS); can damage DNA, protein, and lipids; and are proposed as a major cause of aging [3–7].

Mitochondrial dysfunction impairs male fertility due to its deleterious effects on spermatogenesis [8–13] and function of spermatozoa [14–21]. The spermatogenic defects observed in mito-mice, which harbor a deletion in mitochondrial DNA (mtDNA) [8], and mice with an mtDNA mutator phenotype [12, 13] clearly demonstrate the importance of normal mitochondrial function in spermatogenesis. Indirect evidence suggests that high levels of ROS also disrupt spermatogenesis. Mice lacking *Nrf2*, a gene encoding a transcription factor that regulates the expression of enzymes important for protection from endogenous ROS, develop impaired spermatogenesis in an age-dependent manner [22]. Low partial pressure of oxygen reduces germ cell apoptosis in human testis [9]. ROS are also involved in spermatogenic damages induced by heat, ischemia-reperfusion, and toxic chemicals [23–27].

Mammalian cells have antioxidant enzymes to detoxify superoxide generated by mitochondria and other sources. Superoxide dismutase 1 (SOD1) and SOD2 both contribute to transforming mitochondria-generated superoxide to hydrogen peroxide [28, 29]. Catalase and various glutathione peroxidases then transform hydrogen peroxide to water. Gene mutagenesis in mice has demonstrated the importance of these antioxidant enzymes in spermatogenesis. For example, SOD1-deficient mice are more sensitive to heat-induced spermatogenic impairment [25]. Furthermore, deletion of the *Gpx4* gene in spermatocytes causes male infertility [30].

The *Gpx4* gene generates three different transcripts from different promoters [31]: a ubiquitously expressed short transcript encoding the cytosolic GPX4 [32]; a long transcript mainly expressed in male germ cells encoding a mitochondrial GPX4 [33]; and a male germ cell-specific transcript containing a different exon and encoding a nuclear/nucleolar GPX4 [34]. The mitochondrial GPX4 (mGPX4) is similar in size to cytosolic GPX4 (cGPX4) when tested using Western blots due to the removal of the mitochondrial targeting sequence [33], while the nuclear/nucleolar GPX4 generates a 34kd full-length protein and several truncated peptides between 20~34kd [35, 36]. The nuclear/nucleolar GPX4 is dispensable for viability and fertility [37], the cytosolic GPX4 is essential for viability and spermatogenesis [30, 38] and the mitochondrial GPX4 is important for normal sperm morphology and male fertility [38, 39].

Although mitochondria are the primary source of intracellular ROS [3], direct evidence of mitochondrial ROS involvement in spermatogenic damage is scant. One reason is that mitochondria are multi-functional and mitochondrial dysfunction usually causes multiple functional defects, such as energy deficiency, membrane potential collapse, elevated ROS generation, and increased apoptosis. All of these processes are intimately related, and one can usually cause and enhance the others. Another reason is that suitable animal models for *in vivo* studies are lacking; knocking out genes necessary for normal mitochondrial function often causes embryonic lethality in mice.

Recently, we reported that mutation of the *Inner Mitochondrial Membrane Peptidase 2-like* (*Immp2l*) gene in mice caused age-dependent spermatogenic defects with increased germ cell apoptosis and impaired the signal peptide sequence processing of both cytochrome c1 and mitochondrial glycerol phosphate dehydrogenase 2 [40]. The mitochondria from mutant mice generate elevated levels of superoxide ions, but lack obvious deficiencies in ATP generation or membrane potential maintenance. The mutants showed erectile dysfunction after they reach sexual maturity [40], and with increasing age, they show abnormal bladder

function [41]; multiple age-associated disorders such as wasting, kyphosis, and ataxia [42]; and age-dependent spermatogenic damage [40].

It is unknown why spermatogenic defects are only observed in older but not in younger mutant mice, although superoxide generation is elevated even in young mutants. The mitochondrial 'vicious cycle' theory of aging posits that mtDNA mutations accumulate progressively during life, leading to enhanced ROS generation. In turn, increased ROS production increases rates of mtDNA damage and mutagenesis [43]. Here, we examine the involvement of ROS stress, antioxidant enzymes, and mtDNA mutation in age-dependent spermatogenic damage of *Immp2l* mutant mice.

Materials and Methods

Animals

The generation of $Immp2l^{Tg(Tyr)979Ove}/Immp2l^{Tg(Tyr)979Ove}$ mutant mice has been described previously [40]. Mice were housed in the pathogen-free animal facility at Wake Forest University Health Sciences. Experiments were conducted in accordance with the National Research Council publication Guide for Care and Use of Laboratory Animals, and approved by the Institutional Animal Care and Use Committee of Wake Forest University Health Sciences. Mice were kept in microisolator cages with 12-h light/dark cycles and were fed *ad libitum*. Genotypes were determined by coat color. Homozygous normal mice are albino due to the FVB background. Heterozygotes are slightly pigmented due to the expression of tyrosinase from one copy of the transgene. Homozygous mutant mice are darkly pigmented due to the expression of tyrosinase from two copies of the transgene. All animals used in this study were progenies of one single pair of breeding mice to minimize individual phenotypic variation and rule out possible mitochondrial DNA heterogeneity.

Testis histology and seminiferous epithelium cycle staging

Testis tissues were fixed in Bouin's fixative at 4°C overnight, processed, and embedded in paraffin. 5–8 μm sections were obtained for hematoxylin and eosin (H&E) and periodic acid-Schiff (PAS) staining. PAS-stained sections were used to determine the stage of the cycle of seminiferous epithelium by morphology of the acrosome in haploid germ cells, as described previously [44]. Russell's staging criteria were used for staging of the seminiferous tubules [45].

Western blotting assay of antioxidant enzyme expression

Testes from males of 2–5 months (with normal spermatogenesis) and 13 months (with impaired spermatogenesis) were collected and snap frozen in liquid nitrogen. They were stored at −80 °C till analyzed. Testicular tissues were lysed in RIPA buffer with protease inhibitors (0.5mM PMSF and 1x Complete Protease Inhibitor Cocktail from Roche) and the extracts from control and age-matched mutant mice (n=5/group) were used for SDS-PAGE and Western blotting analyses. Mitochondrial and cytosolic proteins were isolated from testicular tissues as described [38]. β-actin was used for loading control of tissue lysates and cytosolic protein, and VDAC1 was used for loading control of mitochondrial protein.

Anti-β-actin antibody was from Sigma and used at 1:5000 (St Louis, MO); antibodies to superoxide dismutase 1 (ab13498, 1:2000) and VDAC1 (ab14734, 1:2000) were from Abcam (Cambridge, MA), antibodies to SOD2 (1:1000), glutathione peroxidase 4 (GPX4, 1:2000) and catalase (1:1000) were from Santa Cruz. Horseradish peroxidase (HRP)-conjugated secondary antibodies (1:1000) were purchased from Pierce (Rockford, IL). Chemiluminescent reagents from Pierce were used to visualize the protein signals using an LAS-3000 imaging system (Fujifilm). The Integrated Density function (Image J software)

was used to quantify the expression of individual proteins after normalized by β-actin. Finally, ANOVA and t-tests were used to compare the expression between control and mutant mice.

Quantitative RT-PCR (qRT-PCR)

Mice were sacrificed by CO_2 overdose and testicular tissues were snap frozen in liquid nitrogen and then stored at −80°C before RNA extraction. Total RNA was extracted with RNeasy Mini Kit (Qiagen) as instructed by the manufacturer. Residual genomic DNA was removed by DNase treatment with a kit from Qiagen. Reverse transcription was performed with the SuperScript™ First-Strand Synthesis System from Invitrogen.

Real-time PCR was performed on a 7300 real-time PCR system (Applied Biosystems). *Ppib* (*PpibF*: tcgtctttggactctttggaa, and *PpibR*: agcgctcaccatagatgctc) was used an internal control. The following primers were designed to detect the expression of different *Gpx4* transcripts: *mGpx4F* (ggcgcatctgaccaataagag) and *Gpx4R* (cacacgaaacccctgtacttatc) for transcripts encoding mitochondrial GPX4; *nGpx4F* (agcccattcctgaacctttc) and *Gpx4R* for transcripts encoding nuclear/nucleolar GPX4; *cmGpx4* (gccgtctgagccgcttac) and *Gpx4R* for transcripts encoding mitochondrial and cytosolic GPX4. All primer pairs span introns and *Gpx4R* pairs with the junction of exon 2 and 3, excluding the possibility of amplification from genomic DNA. SYBR Green PCR Master Mix (Applied Biosystems) was used for real-time PCR. After the PCR amplification, a dissociation program was run and the amplified product was analyzed by electrophoresis to verify the specificity of the amplification. Relative gene expression levels were calculated using the ΔΔCT method [46]. Equal amount cDNA from five animals of each group was pooled to be used as template for real-time PCR. Three independent experiments were performed with each experiment in triplicate assay. Results were presented as mean ± SEM.

ELISA for protein carbonyl content

Testes were homogenized in Tris-buffered saline lysis buffer (10 mmol/L Tris.HCI pH7.2, 0.5% Triton X-100, 50 mmol/L NaCI, 1 mmol/L EDTA) with protease inhibitors (1x Complete Protease Inhibitor Cocktail from Roche) and centrifuged at 16,000g for 5 minutes at 4 °C and the protein concentration of the supernatant was measured using a Biuret protein assay. Samples were adjusted to 6 mg/ml by dilution with Tris-buffered saline, and protein carbonyl content was determined by a protein carbonyl enzyme immune-assay kit from BioCell Corp according to the instruction of the manufacturer. Data were analyzed by analysis of variance (ANOVA) followed by Bonferroni post-tests.

Testicular germ cell population separation by BSA gradient

Male control and mutant mice aged 11–12 months were used for germ cell isolation by BSA gravity sedimentation. The procedures described by Bellve [47, 48] were followed. Briefly, mice were sacrificed by CO_2 overdose and the testes were dissected free of fat. The seminiferous tubules were sequentially digested by collagenase and trypsin. The tissue was pipetted briefly and gently to disperse the cells. After passage through an 80 μm mesh filter, the cells were resuspended in buffer containing 0.5% BSA and loaded in a STA-PUT velocity sedimentation cell separator (ProScience Inc.) for gradient separation. Fractions containing the same cell type were combined and cells collected by centrifuge at 500 g for 10 min. Three germ cell populations (spermatocytes, round spermatids, and elongated spermatids) were collected for subsequent analysis. Cell type was determined by observing morphological features under differential interference contrast light microscopy. Judged by cell morphology, cell purity was estimated at 85%.

Flow cytometry analysis of apoptotic testicular cells

Testes were collected from 13-month-old mice sacrificed by carbon dioxide overdose, and testicular cells were isolated as described previously [44, 49]. Apoptotic cells were labeled by *In Situ* Cell Death Detection Kit, Fluorescein (Roche), following the manufacturer's instructions. Cells were then treated with 40 μg/ml RNase A and stained with 25 μg/ml propidium iodide in PBS. The cells were then analyzed by flow cytometry with a BD FACSCalibur analyzer. Data were analyzed by analysis of variance (ANOVA), followed by Bonferroni post-tests.

Detection of De novo germ cell mtDNA mutation

Total genomic DNA was isolated from spermatocytes, round spermatids, and elongated spermatids using the DNeasy Blood & Tissue kit (Qiagen). *De novo* mutations in two regions of the mitochondrial genome were surveyed: region 1 spans nt 5495 and 5981 (numbered according to NCBI Reference Sequence NC_005089.1) and is within the cytochrome c oxidase (*mt-Co1*) gene; region 2 spans nt 15196 and nt 15720 and contains the cytochrome b (*mt-Cytb*) gene and the D-loop control region. These regions were chosen to facilitate comparison with earlier studies [12, 13]. DNA of the two regions was amplified by High Fidelity PCR Master (Roche) with the following two pairs of primers: MitF (GCCAACTAGCCTCCATCTCATACTT, nt 15196–15220) and MitR (GGGCGGGTTGTTGGTTTCAC, nt 15701–15720), MitF1 (TATCGTAACTGCCCATGCTTTTGT, nt 5495–5518) and MitR1 (AGTTGTGTTTAGGTTGCGGTCTGT, nt 5958–5981). The cycling conditions were: 94°C for 4 min, followed by 35 cycles of 94°C for 30 sec, 55°C for 30 sec, and 72°C for 30 sec. PCR products were cloned into the pCR4-TOPO™ vector using a TOPO™ TA Cloning Kit (Invitrogen). 60–90 colonies from mutant and control DNA were grown and plasmid DNA was isolated using the Qiaprep Turbo 96 Mini-prep Kit (Qiagen). Plasmid DNA was sequenced using T3 and T7 primers. The frequency of PCR and cloning-induced mutations was determined by reamplifying, cloning, and sequencing 50 individual clones. This rate was subtracted from the observed mutational data to determine the mtDNA mutation rate for control and mutant mice.

Detection of germ cell mtDNA deletion

Long-range nested PCR was used to detect possible mtDNA deletion in elongated spermatids. Two regions (nt 15196-5981 and nt 5495–12876), covering 14kb of the 16.3kb mouse mitochondrial genome, were amplified to detect possible deletions in these regions. To amplify region 5495–12876 (region 1 in Fig.5A), MitF1 and MitR were used to amplify region 5495–12876, then MitF1 and ND5R (CGAGGCTTCCGATTACTAGG, nt 12876-12857) were used in semi-nested PCR to amplify DNA from region 5495-12876. To amplify region 15196-5981 (region 2 in Fig. 5A), ND5F (CTGGCAGACGAACAAGACATC, nt 12789–12809) and MitR1 were used to amplify region 12789-5981, then MitF and MitR1 were used in semi-nested PCR to amplify DNA from region 15196-5981. Long-range PCR was performed with the Expand Long Range dNTPack (Roche) according to the manufacturer's instructions. Amplification products were separated by electrophoresis on a 0.8% agarose gel (containing 0.5 μg/ml ethidium bromide) and observed under UV light.

Detection of germ cell mtDNA content

Quantitative PCR (qPCR) was used to compare the mtDNA content in spermatocytes and round spermatids of mutants and controls. ND5F and ND5R primers amplifying an 87 bp region of the *mt-Nd5* gene were used to amplify the mtDNA. 18sRNA Taqman probe (Applied Biosystems) and *Gapdh* primers, which gave similar results in qPCR, were used

for amplifying genomic DNA. Sybr Green and Taqman 2xPCR mixtures (Applied Biosystems) were used for qPCR. qPCR was performed using the ABI PRISM 7700 Sequence Detector (Applied Biosystems). The PCR cycling conditions were: initial denaturation at 95 °C for 10 min, followed by 40 cycles of 95°C for 30 s, then 60°C for 1 min. The mtDNA/nDNA ratio was derived from the difference in threshold cycle value (ΔCt) between *mt-Nd5* and 18S rRNA, using the $2^{-\Delta Ct}$ method [46]. Triplicate assays were performed for each sample. All experiments were repeated at least once. Results are presented as means ± SEM.

Results

Time course of spermatogenic damage in Immp2l mutant males

No difference in spermatogenesis was observed in control and mutant mice at 5 weeks (when the first batch of elongated spermatozoa are released from the seminiferous tubules [50]) (Fig.1A, B). Furthermore, spermatozoa were observed in the epididymis of control and mutant mice (data not shown), indicating that the mutation does not affect spermatogenic development in prepubertal mutants. Spermatogenesis was qualitatively normal in mutant males up to the age of 10 months (Fig.1C–F). However, beyond that point, 100% of the mutant mice examined showed germ cell deficiency and disorganization in over 30% of the seminiferous tubules (Fig.1H, I; Table 1). Control mice showed normal spermatogenesis even at the age of 15 months (Fig.1J).

Of 23 mutant mice between 11 and 15 months old, only 4 (18%) showed germ cell deficiency in over 80% of the seminiferous tubules (Table 1). The remaining mutant mice showed only moderate germ cell deficiency in 30%–50% of the seminiferous tubules, although none of the control mice showed similar germ cell deficiency at that age. The earliest time to observe spermatogenic damage in these mutants is 4 months later than originally reported [40], and the degree of spermatogenic damage tends to be less severe than originally observed. Possible explanations for these findings include: 1) all animals used after the original publication were progenies of one single pair of breeding mice, to minimize individual variation and eliminate mitochondrial DNA heterogeneity; 2) mice described in [40] were bred at the animal facility of Baylor College of Medicine and transferred to WFUHS; different housing conditions and possible stress of moving may have affected the timing and severity of spermatogenic damage. *Immp2l* mutant mice 11 to 15 months old have seminal vesicles of normal sizes (data not shown); therefore, their impaired spermatogenesis is not caused by androgen suppression.

Apoptosis was increased in mutants with spermatogenic damage independent of testicular cell type

To examine the testicular cell populations affected by the mutation, testicular cells of 13-month-old mutant males were isolated, labeled by propidium iodide, and analyzed by flow cytometry. Based on propidium iodide binding capacity, the following testicular cell populations were recognized: HC, hypo-stained elongating and elongated spermatids; 1C, round spermatids; 2C, spermatogonia, secondary spermatocytes and somatic cells; 4C, primary spermatocytes and G2 spermatogonia; and S-ph, spermatogonia and preleptotene spermatocytes synthesizing DNA (Fig. 2A). We considered S-ph cells primarily as germ cells, since the proportion of somatic cells (Sertoli, Leydig and other nongerm cells) is less than 3% of total testicular cells in normal mouse testis [51], and at this age most somatic cells are post-mitotic and will not synthesize DNA.

Spermatogenic impairment was confirmed by histological analysis of testicular tissues. Germ cell deficiency was consistent with a significantly reduced number of testicular cells

isolated from mutant mice ($11.8\times10^6 \pm 1.8\times10^6$/testis, n=5 for controls; $4.0\times10^6 \pm 1.1\times10^6$/testis, n=4 for mutants; $p<0.05$). While the percentage of spermatids (including HC and 1C cells) differed between control and mutant mice, the percentage of other cell populations (2C, S-ph and 4C cells) did not (Fig. 2B).

Flow cytometry analysis of TUNEL-labeled testicular cells of 13-month-old control and mutants showed that mutants had a significantly higher percentage of TUNEL-positive cells (Fig. 2C, column "total"), explaining the significantly reduced numbers of testicular cells in the mutants. In addition, 1C, 2C, S-ph and 4C cells all showed higher percentages of TUNEL-positive cells in mutants than in controls (Fig. 2C), suggesting that all testicular cell populations were affected in mutant mice. Spermatogonia and preleptotene spermatocytes synthesizing DNA had the highest percentage of TUNEL-positive cells (S-ph, Fig. 2C), suggesting that spermatogonia are likely to be affected by excessive ROS in mutants. This is consistent with our recent observation of adult stem cell damage in aged *Immp2l* mutant mice [42]. Higher percentages of TUNEL-positive testicular cells from mutant mice indicated a greater incidence of apoptosis. Apoptosis may not be involved in the death of mouse spermatozoa [52]. We observed a higher percentage of TUNEL-positive elongating and elongated spermatids in mutants than in controls (1.6% ± 0.4%, n=5 for controls; 6.1% ± 1.2%, n=4 for mutants, $p<0.05$), which may result from a higher incidence of genomic DNA damage in these cells in mutants.

Spermatogenic stages at which the germ cells are affected were further analyzed histologically. Testicular sections from mutant mice were stained with periodic acid-Schiff (PAS) and cross-sections of tubules with obvious germ cell deficiency were staged for qualitative analyses. Staging was based on acrosome morphology (red stain after PAS staining). This analysis confirmed germ cell deficiency in old mutant mice and that germ cell deficiency was not cell type-specific (Fig. 2D). For example, while step 9, 13, and 15 spermatids were readily visible in control mice, they were reduced in affected seminiferous tubules of mutant mice. Round spermatids and spermatocytes were also reduced in seminiferous tubules from mutant males, based on the reduced number of layers containing these cells.

Elevated oxidative stress was observed in testes of old but not young mutants

Previously, we observed elevated superoxide generation by isolated mitochondria and increased apoptotic germ cells in aged mutant testes, and proposed that the resultant ROS stress underlies age-dependent spermatogenic impairment [40]. If so, aged mutants should show elevated oxidative stress. A sensitive ELISA assay was used to compare amounts of protein carbonyl (an index of oxidative stress) in control and mutant testicular protein before and after spermatogenic damage. Protein carbonyl did not differ between young (2–4 months) control and mutant mice, but was significantly elevated in 13-month-old mutants, which also had impaired spermatogenesis (Fig. 3A). This observation is consistent with age-specific spermatogenic damage.

Cytosolic GPX4 expression was significantly decreased in testis of old mutant males

We examined the expression of the major antioxidant enzymes, SOD1, SOD2, catalase and glutathione peroxidase 4 (a major glutathione peroxidase in the testis), in testes of mutant and control mice by Western blotting. Both in 2- to 5-month-old mutants with normal spermatogenesis (Fig. 3B), and in 13-month-old mutant and control mice (Fig. 3C), SOD1 and SOD2 expression did not differ from that in age-matched controls; however, catalase expression was increased in mutant mice in both age groups. In control and mutant males, catalase expression also increased significantly with age (Fig. 3D).

The testis expresses three isoforms of GPX4: the nuclear/nucleolar GPX4 (nGPX4), cytosolic GPX4 (cGPX4) and mitochondrial GPX4 (mGPX4). We compared the expression of the GPX4 isoforms in testis of mutant and control mice. Several groups have demonstrated that nGPX4 produces several truncated products smaller than the 34 kD full-length protein [35, 36]. Thus, we interpreted bands of >20 kD in Fig. 4A–C (marked by "n") as being truncated products of nGPX4. The intensity of these bands did not differ between controls and mutants, nor between young and old mice. cGPX4 and mGPX4 are indistinguishable in Western blotting due to the processing of the presequence from mGPX4. The combined product of cGPX4 and mGPX4 (indicated by "c+m" in Fig. 4) was significantly decreased in mutants compared with age-matched controls (Fig. 4A, B, D). Even in control mice, c+mGPX4 decreased significantly in old mice compared with 2- to 5-month-old mice (Fig. 4C, E). Since our flow cytometry analysis showed that 13-month-old mutant and control mice had similar percentages of HC+1C (expressing nGPX4), 2C, S-ph and 4C cells (Fig. 2B), different c+mGPX4 expression was not attributable to different germ cell composition and was the result of reduced expression of c+mGPX4 protein *per se*.

To examine whether reduced c+mGPX4 in mutant mice is caused by reduction in cGPX4, mGPX4, or both, we isolated sytosolic and mitochondrial protein from testes of 13- to 14-month–old males. While mGPX4 showed only a slight reduction in mutant mice, cGPX4 showed a much greater reduction (Fig. 4F). The data demonstrated that cGPX4 decreased significantly in old mutant mice with impaired spermatogenesis.

Real-time RT-PCR was performed to further examine the expression of different *Gpx4* transcripts at the mRNA level. Primers were designed to compare the expression of *nGpx4*, *mGpx4*, and *c+mGpx4* between control and mutant males (Fig. 4G). Primers are unavailable to detect only *cGpx4*, since they will also amplify from *mGpx4* transcripts. All the primers were demonstrated to be specific by one single peak in dissociation curves and by a single amplicon of the expected size. mRNA levels of different *Gpx4* transcripts could not explain the levels of corresponding GPX4 protein isoforms. While *nGpx4* decreased significantly in 13-month-old mutants compared with young mice and 13-month-old controls (Fig. 4H), nGPX4 protein did not differ among different groups (Fig. 4A–C). On the contrary, while *mGpx4* and *c+mGpx4* showed no significant difference between 2-~5-month-old control and mutants (Fig. 4H), c+mGPX4 protein expression decreased 50% in 2-~5-month-old mutants (Fig. 4A, D). In addition, compared with 13-month-old control mice, 13-month-old mutant mice showed a greater degree of decrease in c+mGPX4 protein (Fig. 4B, D) than in *c+mGpx4* mRNA (Fig. 4H). A similar contrast was also observed when comparing young and old control mice, in that *c+mGpx4* mRNA showed no significant age-related difference while c+mGPX4 protein showed a 4-fold difference (Fig. 4C, E). The data suggest that post-transcriptional regulation plays a major role in the expression of different GPX4 isoforms.

mtDNA mutation is not involved in spermatogenic defects in aged mutant mice

mtDNA mutation causes spermatogenic damage [8, 12, 13]. Elevated mitochondrial superoxide generation and increased levels of oxidative stress in *Immp2l* mutant testis prompted us to test whether elevated mitochondrial superoxide generation causes spermatogenic damage by increasing the mtDNA mutation rate, as proposed by the mitochondrial 'vicious cycle' theory of aging [43]. We compared the mtDNA mutation rate in elongated spermatids isolated from 11-month-old control and mutant males using the BSA gradient method. This age was chosen because histologic analysis revealed that spermatogenesis in all mutant mice of this age is impaired.

DNA fragments containing nt 15196–15720, which contains the *mt-Cytb* gene and the D-loop control region, and nt 5495–5981, which contains the *mt-Co1* gene (Fig.5A), were amplified by high-fidelity PCR using total DNA isolated from elongated spermatids. These

DNA fragments were subcloned and sequenced. Possible mtDNA mutations arising during PCR and subcloning were subtracted from the observed mutation rates. DNA sequenced for region 15196–15720 was 27.3 kb for control and 28.3 kb for mutant mice; DNA sequenced for region 5495–5981 was 33.6 kb for control and 40.3 kb for mutant mice. When both regions were considered, 60.9 kb was sequenced for control and 68.6 kb was sequenced for mutant mice. We found 3.13 mutations/10 kb for control mice and 3.22 mutations/10 kb for mutant mice (Fig. 5B), agreeing with published observation of 2–6 mutations/10 kb mtDNA [12, 13], and suggesting no significant difference in the mtDNA mutation rate between control and mutant males

Analyses of the mtDNA mutation type revealed no insertions or deletions in control and mutant mice. In both types, the predominant point mutations were transitions (30/31 for mutants and 26/27 for controls). Thus, our data strongly suggest that mtDNA point mutation is not involved in the spermatogenic defects observed in old mutant mice.

To examine whether large mtDNA deletions are involved in the spermatogenic defects in old mutant mice, we compared mtDNA deletions in elongated spermatids by long- range PCR. We performed semi-nested PCR to amplify two regions of mouse mtDNA: 5495–12876 (product 1 in Fig. 5A), and 15196-5981 (product 2 in Fig. 5A), which cover 13979 bp (85.8%) of the 16299 bp mouse mitochondrial genome. No increase in shorter amplified products (resulting from mtDNA deletion) was observed in PCR products from either region of mutant males, indicating no increased mtDNA deletion in old mutants (Fig. 5C).

For an unknown reason, region 2 was more difficult to amplify from mutant DNA in long-range PCR, so fewer full-length PCR products were obtained from mutant DNA in the first round of PCR. This was not caused by a lower DNA input, since the template DNA was equal and region 1 was efficiently amplified from mutant DNA. To address this issue, we recovered all possible amplified DNA except the dominant full-length PCR product from the first PCR by gel purification (Fig. 5C, boxed region), and used this DNA as the template for the second round of PCR (Fig. 5C, Recovered). This time, similar cohorts of short PCR products were found in PCR products from control and mutant animals, confirming no increase of mtDNA deletion in mutant animals.

Quantitative PCR was used to examine whether isolated spermatocytes and round spermatids from mutant males had reduced mtDNA content. Based on cell morphology, the purity of both cell populations was estimated at 85%. Elongated spermatids were excluded from analyses due to heterogeneity of the cell population. Primers specific to *mt-Nd5* were used to quantify mtDNA content, and 18s rRNA primers were used to control genomic DNA input. Neither spermatocytes nor round spermatids from mutants had less mtDNA (Fig. 5D). The *mt-Nd5* gene is located in region 1, and PCR amplification of this region from mutant mtDNA is efficient in long-range PCR. This comparison is unlikely to be affected by the possible difference in amplification efficiency between control and mutant mtDNA. Indeed, even if the amplification of *mt-Nd5* DNA from mutant mice were less efficient, it would reinforce the argument that mtDNA content in mutant germ cells is not reduced. Thus, these data indicate that mtDNA mutation is not involved in spermatogenic impairment in aged mutant mice.

Discussion

The present report refined the time course of spermatogenic impairment in a new cohort of *Immp2l* mutant males and examined the possible involvement of oxidative stress and mtDNA mutation in age-dependent spermatogenic impairment of the mutants. Following our previous finding that mitochondria from mutant testes generate more superoxide [40],

we found elevated protein carbonyl content in testes of 13-month-old but not 2- to 5-month-old mutants. This observation confirmed increased oxidative stress in *Immp2l* mutant mice, and supported the linkage between high oxidative stress and spermatogenic damage. We found that 2- to 5-month-old mutant mice had normal levels of oxidative stress and normal spermatogenesis; whereas 13-month-old mutant mice had both elevated oxidative stress and impaired spermatogenesis. While it remains unclear why oxidative stress is elevated in old but not young mutants, and whether elevated oxidative stress is the cause or a co-occurring event, our data strongly support the role of oxidative stress in this process.

Our results regarding antioxidant enzyme expression also implicate ROS in spermatogenesis of mutant mice. We observed elevated catalase expression in young and old mutants, although impaired spermatogenesis damage was seen only in old mutants. Since hydrogen peroxide induces catalase expression [53], increased catalase expression is most likely a feedback response to increased hydrogen peroxide transformed by SOD1 and SOD2 from excessive mitochondrial superoxide levels in mutant mice. Testicular cells express high levels of SOD1 and SOD2 [54, 55], which might be sufficient to detoxify elevated superoxide from mutant mitochondria. This could also explain why SOD1 and SOD2 expression in testes of mutant mice is not different from control mice.

GPX4 specifically metabolizes lipid peroxides and is highly expressed in germ cells [56], and it is essential for normal spermatogenesis [30, 38]. Testicular cells express three GPX4 isoforms, cGPX4, mGPX4, and nGPX4 (restricted to round and elongated spermatids). While nGPX4 did not show significant differences between control and mutant mice, testicular c+mGPX4 of 2- to 5-month-old mutant mice was 50% of age-matched normal mice, and that of 13-month-old mutants was 33% of age-matched controls. Further experiments demonstrated that cGPX4 reduction contributed much more than mGPX4 in the reduction of c+mGPX4. Considering the fact that testicular c+mGPX4 expression (and most likely cGPX4 too) in normal 13-month-old males is greatly decreased compared with young males, a greater decrease of cGPX4 expression in 13-month-old mutants than in age-matched controls may have caused cGPX4 deficiency. nGPX4 is dispensable for spermatogenesis and fertility [37], mGPX4 is important for normal sperm morphology and function but not important for normal spermatogenesis [39], and cGPX4 is necessary for normal spermatogenesis [30, 38]. Decreased cGPX4 expression in testes of 13-month-old mutants might be one of the mechanisms underlying the age-dependent spermatogenic damage. While cGPX4 reduction might be one of the mechanisms explaining the spermatogenic damages of old mutant mice, it is the secondary result of the primary cause: increased production of superoxide by mutant mitochondria. It has been shown in somatic tissues that *mGpx4* mRNA translational regulation by GRSF1 and DJ-1 plays a critical role in determining the translation efficiency of this mRNA [57, 58]. Consistent with this, our data suggest that post-transcriptional regulation played a major role in determining the expression of different GPX4 isoforms. Learning how cGPX4 expression is inhibited in mutant mice will greatly improve our understanding of the relationship between ROS and *Gpx4* expression.

We found that apoptosis (judged by detection of DNA breaks through TUNEL labeling) was increased in 1C (round spermatids), 2C (secondary spermatocytes, spermatogonia and somatic cells), cells synthesizing DNA, and 4C cells (spermatocytes), suggesting that oxidative damage is not cell type-specific. Although androgen suppression is unlikely a factor (since seminal vesicles were normal in size) in old mutants, the involvement of Sertoli cells and Leydig cells in the observed spermatogenic damage remains to be determined. The increased apoptosis we observed in testicular cells without cell type specificity agrees with our previous report of multiple age-associated phenotypes, including kyphosis, ataxia, and wasting, in mutants starting from the age of 12 months [42]. IMMP2L is one of the two

subunits of inner membrane peptidase (IMP) and is expressed in the testis, ovary, and somatic organs. The involvement of ROS damage in age-dependent spermatogenic impairment reinforces our argument that ROS also underlie age-dependent damage in somatic organs [42].

The mitochondrial 'vicious cycle' theory of aging [43] prompted us to test whether mtDNA mutation could be involved in spermatogenic disruption of *Immp2l* mutants. Although spermatogenesis is impaired in 11-month-old *Immp2l* mutant males, they do not have an increased number of mtDNA mutations (either point mutations or deletions) in their germ cells. In addition, the mtDNA content is not decreased. These data strongly argue against a role for mtDNA mutation in the observed spermatogenic defects in aged *Immp2l* mutants. A recent study examined the relationship of ROS and mtDNA mutation in hematopoetic stem cells, and saw no positive relationship between the levels of ROS and the mtDNA mutation rate [59]. Consistent with that observation, we now provide direct evidence that elevated ROS stress does not necessary result in an increased mtDNA mutation rate. Thus, ROS appear to mediate spermatogenic disruptions in aged *Immp2l* mice without mtDNA mutation. However, due to the limited quantity of DNA obtained from the BSA-separated germ cells, we did not address whether mtDNA from mutant mice contained increased levels of other types of DNA modifications which could affect gene expression from mtDNA.

The strength of the present study is that these observations are based on a genetic model with a defined mitochondrial functional defect (increased superoxide generation). Previous studies examining ROS and spermatogenesis were either retrospective [60, 61] or based on indirect evidence [9, 62]. ROS scavenging enzymes have been manipulated to increase or decrease the rate of ROS clearance, but these efforts do not always generate suitable models for the study of ROS and spermatogenesis. For example, male *Sod1*$^{-/-}$ mice are fertile [63] and *Sod2*$^{-/-}$ mice die within 3 weeks after birth [64, 65]. The *Immp2l* mutation model provides a meaningful opportunity to examine the causal role of mitochondrial ROS in the disruption of spermatogenesis.

The knowledge obtained from this study will improve our understanding and treatment of male infertility associated with environmental toxins, cryptorchidism, testicular torsion/detorsion, diabetes and increased age; ROS have been implicated in all of these situations [25, 26, 66–68]. Establishing a firm link between oxidative stress and spermatogenesis will help us understand and address the testicular consequences of non-reproductive diseases. In conclusion, the present report demonstrates that oxidative stress and antioxidant enzymes, but not mtDNA mutation, are involved in age-dependent spermatogenic impairment in *Immp2l* mutant mice.

Acknowledgments

The authors wish to thank Dr. Yu Zhou (Institute for Regenerative Medicine, Wake Forest University Health Sciences) for help with flow cytometry analysis, Ms. Karen Klein (Research Support Core, Office of Research, Wake Forest University Health Sciences) for editing the manuscript, and Dr. Anthony J. Molina for providing VADC antibody. This work was supported by the National Institutes of Health (R01HD058058 to B. L.).

References

1. Babcock DF, Herrington J, Goodwin PC, Park YB, Hille B. Mitochondrial Participation in the Intracellular Ca2+ Network. J Cell Biol. 1997; 136:833–844. [PubMed: 9049249]
2. Gogvadze V, Orrenius S, Zhivotovsky B. Multiple pathways of cytochrome c release from mitochondria in apoptosis. Biochimica et Biophysica Acta (BBA) - Bioenergetics. 2006; 1757:639–647.

3. Andreyev AY, Kushnareva YE, Starkov AA. Mitochondrial metabolism of reactive oxygen species. Biochemistry (Mosc). 2005; 70:200–214. [PubMed: 15807660]
4. Sedensky MM, Morgan GP. Mitochondrial respiration and reactive oxygen species in mitochondrial aging mutants. Experimental Gerontology. 2006; 41:237–245. [PubMed: 16497463]
5. Madamanchi NR, Runge MS. Mitochondrial Dysfunction in Atherosclerosis. Circ Res. 2007; 100:460–473. [PubMed: 17332437]
6. Harman D. Aging: a theory based on free radical and radiation chemistry. J Gerontol. 1956; 11:298–300. [PubMed: 13332224]
7. Harman D. The biologic clock: the mitochondria? J Am Geriatr Soc. 1972; 20:145–147. [PubMed: 5016631]
8. Nakada K, Sato A, Yoshida K, Morita T, Tanaka H, Inoue S, Yonekawa H, Hayashi J. Mitochondria-related male infertility. Proc Natl Acad Sci U S A. 2006; 103:15148–15153. [PubMed: 17005726]
9. Erkkila K, Pentikainen V, Wikstrom M, Parvinen M, Dunkel L. Partial oxygen pressure and mitochondrial permeability transition affect germ cell apoptosis in the human testis. J Clin Endocrinol Metab. 1999; 84:4253–4259. [PubMed: 10566681]
10. Ishii N, Fujii M, Hartman PS, Tsuda M, Yasuda K, Senoo-Matsuda N, Yanase S, Ayusawa D, Suzuki K. A mutation in succinate dehydrogenase cytochrome b causes oxidative stress and ageing in nematodes. Nature. 1998; 394:694–697. [PubMed: 9716135]
11. Kayser E-B, Sedensky MM, Morgan PG. The effects of complex I function and oxidative damage on lifespan and anesthetic sensitivity in Caenorhabditis elegans. Mechanisms of Ageing and Development. 2004; 125:455–464. [PubMed: 15178135]
12. Trifunovic A, Wredenberg A, Falkenberg M, Spelbrink JN, Rovio AT, Bruder CE, Bohlooly-Y M, Gidlof S, Oldfors A, Wibom R, Tornell J, Jacobs HT, Larsson N-G. Premature ageing in mice expressing defective mitochondrial DNA polymerase. Nature. 2004; 429:417–423. [PubMed: 15164064]
13. Kujoth GC, Hiona A, Pugh TD, Someya S, Panzer K, Wohlgemuth SE, Hofer T, Seo AY, Sullivan R, Jobling WA, Morrow JD, Van Remmen H, Sedivy JM, Yamasoba T, Tanokura M, Weindruch R, Leeuwenburgh C, Prolla TA. Mitochondrial DNA Mutations, Oxidative Stress, and Apoptosis in Mammalian Aging. Science. 2005; 309:481–484. [PubMed: 16020738]
14. de Lamirande E, Gagnon C. Reactive oxygen species and human spermatozoa. I. Effects on the motility of intact spermatozoa and on sperm axonemes. J Androl. 1992; 13:368–378. [PubMed: 1331006]
15. Kim JG, Parthasarathy S. Oxidation and the spermatozoa. Semin Reprod Endocrinol. 1998; 16:235–239. [PubMed: 10101805]
16. Iwasaki A, Gagnon C. Formation of reactive oxygen species in spermatozoa of infertile patients. Fertil Steril. 1992; 57:409–416. [PubMed: 1735495]
17. Fabio FP, Rakesh KS, David RN, Anthony JT, Ashok A. Relationship between oxidative stress, semen characteristics, and clinical diagnosis in men undergoing infertility investigation. Fertility and sterility. 2000; 73:459–464. [PubMed: 10688996]
18. Wang X, Sharma RK, Gupta A, George V, Thomas AJ, Falcone T, Agarwal A. Alterations in mitochondria membrane potential and oxidative stress in infertile men: a prospective observational study. Fertility and Sterility. 2003; 80:844–850. [PubMed: 14505763]
19. Ruiz-Pesini E, Diez C, Lapena AC, Perez-Martos A, Montoya J, Alvarez E, Arenas J, Lopez-Perez MJ. Correlation of sperm motility with mitochondrial enzymatic activities. Clin Chem. 1998; 44:1616–1620. [PubMed: 9702947]
20. Alvarez JG, Storey BT. Role of glutathione peroxidase in protecting mammalian spermatozoa from loss of motility caused by spontaneous lipid peroxidation. Gamete Res. 1989; 23:77–90. [PubMed: 2545584]
21. Koppers AJ, De Iuliis GN, Finnie JM, McLaughlin EA, Aitken RJ. Significance of mitochondrial reactive oxygen species in the generation of oxidative stress in spermatozoa. J Clin Endocrinol Metab. 2008; 93:3199–3207. [PubMed: 18492763]
22. Nakamura BN, Lawson G, Chan JY, Banuelos J, Cortés MM, Hoang YD, Ortiz L, Rau BA, Luderer U. Knockout of the transcription factor NRF2 disrupts spermatogenesis in an age-

dependent manner. Free Radical Biology and Medicine. 2010; 49:1368–1379. [PubMed: 20692336]

23. Ikeda M, Kodama H, Fukuda J, Shimizu Y, Murata M, Kumagai J, Tanaka T. Role of radical oxygen species in rat testicular germ cell apoptosis induced by heat stress. Biol Reprod. 1999; 61:393–399. [PubMed: 10411517]
24. Lysiak JJ, Zheng S, Woodson R, Turner TT. Caspase-9-dependent pathway to murine germ cell apoptosis: mediation by oxidative stress, BAX, and caspase 2. Cell Tissue Res. 2007; 328:411–419. [PubMed: 17265069]
25. Ishii T, Matsuki S, Iuchi Y, Okada F, Toyosaki S, Tomita Y, Ikeda Y, Fujii J. Accelerated impairment of spermatogenic cells in sod1-knockout mice under heat stress. Free Radical Research. 2005; 39:697–705. [PubMed: 16036348]
26. Turner TT, Tung KS, Tomomasa H, Wilson LW. Acute testicular ischemia results in germ cell-specific apoptosis in the rat. Biol Reprod. 1997; 57:1267–1274. [PubMed: 9408230]
27. Chaki SP, Misro MM, Gautam DK, Kaushik M, Ghosh D, Chainy GB. Estradiol treatment induces testicular oxidative stress and germ cell apoptosis in rats. Apoptosis. 2006; 11:1427–1437. [PubMed: 16830234]
28. Han D, Antunes F, Canali R, Rettori D, Cadenas E. Voltage-dependent Anion Channels Control the Release of the Superoxide Anion from Mitochondria to Cytosol. Journal of Biological Chemistry. 2003; 278:5557–5563. [PubMed: 12482755]
29. Okado-Matsumoto A, Fridovich I. Subcellular Distribution of Superoxide Dismutases (SOD) in Rat Liver. Journal of Biological Chemistry. 2001; 276:38388–38393. [PubMed: 11507097]
30. Imai H, Hakkaku N, Iwamoto R, Suzuki J, Suzuki T, Tajima Y, Konishi K, Minami S, Ichinose S, Ishizaka K, Shioda S, Arata S, Nishimura M, Naito S, Nakagawa Y. Depletion of selenoprotein GPx4 in spermatocytes causes male infertility in mice. J Biol Chem. 2009; 284:32522–32532. [PubMed: 19783653]
31. Maiorino M, Scapin M, Ursini F, Biasolo M, Bosello V, Flohe L. Distinct promoters determine alternative transcription of gpx-4 into phospholipid-hydroperoxide glutathione peroxidase variants. J Biol Chem. 2003; 278:34286–34290. [PubMed: 12819198]
32. Brigelius-Flohe R, Aumann KD, Blocker H, Gross G, Kiess M, Kloppel KD, Maiorino M, Roveri A, Schuckelt R, Usani F, et al. Phospholipid-hydroperoxide glutathione peroxidase. Genomic DNA, cDNA, and deduced amino acid sequence. J Biol Chem. 1994; 269:7342–7348. [PubMed: 8125951]
33. Arai M, Imai H, Sumi D, Imanaka T, Takano T, Chiba N, Nakagawa Y. Import into mitochondria of phospholipid hydroperoxide glutathione peroxidase requires a leader sequence. Biochem Biophys Res Commun. 1996; 227:433–439. [PubMed: 8878533]
34. Pfeifer H, Conrad M, Roethlein D, Kyriakopoulos A, Brielmeier M, Bornkamm GW, Behne D. Identification of a specific sperm nuclei selenoenzyme necessary for protamine thiol cross-linking during sperm maturation. Faseb J. 2001; 15:1236–1238. [PubMed: 11344099]
35. Puglisi R, Maccari I, Pipolo S, Conrad M, Mangia F, Boitani C. The nuclear form of glutathione peroxidase 4 is associated with sperm nuclear matrix and is required for proper paternal chromatin decondensation at fertilization. J Cell Physiol. 2012; 227:1420–1427. [PubMed: 21618532]
36. Maiorino M, Mauri P, Roveri A, Benazzi L, Toppo S, Bosello V, Ursini F. Primary structure of the nuclear forms of phospholipid hydroperoxide glutathione peroxidase (PHGPx) in rat spermatozoa. FEBS Lett. 2005; 579:667–670. [PubMed: 15670826]
37. Conrad M, Moreno SG, Sinowatz F, Ursini F, Kolle S, Roveri A, Brielmeier M, Wurst W, Maiorino M, Bornkamm GW. The nuclear form of phospholipid hydroperoxide glutathione peroxidase is a protein thiol peroxidase contributing to sperm chromatin stability. Mol Cell Biol. 2005; 25:7637–7644. [PubMed: 16107710]
38. Liang H, Yoo SE, Na R, Walter CA, Richardson A, Ran Q. Short form glutathione peroxidase 4 is the essential isoform required for survival and somatic mitochondrial functions. J Biol Chem. 2009; 284:30836–30844. [PubMed: 19744930]
39. Schneider M, Forster H, Boersma A, Seiler A, Wehnes H, Sinowatz F, Neumuller C, Deutsch MJ, Walch A, Hrabe de Angelis M, Wurst W, Ursini F, Roveri A, Maleszewski M, Maiorino M,

Conrad M. Mitochondrial glutathione peroxidase 4 disruption causes male infertility. Faseb J. 2009; 23:3233–3242. [PubMed: 19417079]

40. Lu B, Poirier C, Gaspar T, Gratzke C, Harrison W, Busija D, Matzuk MM, Andersson K-E, Overbeek PA, Bishop CE. A Mutation in the Inner Mitochondrial Membrane Peptidase 2-Like Gene (Immp2l) Affects Mitochondrial Function and Impairs Fertility in Mice. Biol Reprod. 2008; 78:601–610. [PubMed: 18094351]
41. Soler R, Fullhase C, Lu B, Bishop CE, Andersson KE. Bladder dysfunction in a new mutant mouse model with increased superoxide--lack of nitric oxide? J Urol. 183:780–785. [PubMed: 20022053]
42. George SK, Jiao Y, Bishop CE, Lu B. Mitochondrial peptidase IMMP2L mutation causes early onset of age-associated disorders and impairs adult stem cell self-renewal. Aging Cell. 2011 (In press).
43. Bandy B, Davison AJ. Mitochondrial mutations may increase oxidative stress: Implications for carcinogenesis and aging? Free Radical Biology and Medicine. 1990; 8:523–539. [PubMed: 2193852]
44. Lu B, Bishop CE. Mouse GGN1 and GGN3, two germ cell specific proteins from the single gene Ggn, interact with mouse POG and play a role in spermatogenesis. J Biol Chem. 2003; 278:16289–16296. [PubMed: 12574169]
45. Russell, LD.; Ettlin, RA.; Sinha Hikim, AP.; Clegg, ED. Histological and Histopathological Evaluation of the Testis. Clearwater, Florida: Cache River Press; 1990.
46. Livak KJ, Schmittgen TD. Analysis of Relative Gene Expression Data Using Real-Time Quantitative PCR and the 2-[Delta][Delta]CT Method. Methods. 2001; 25:402–408. [PubMed: 11846609]
47. Bellve AR, Cavicchia JC, Millette CF, O'Brien DA, Bhatnagar YM, Dym M. Spermatogenic cells of the prepuberal mouse. Isolation and morphological characterization. J Cell Biol. 1977; 74:68–85. [PubMed: 874003]
48. Bellve AR. Purification, culture, and fractionation of spermatogenic cells. Methods Enzymol. 1993; 225:84–113. [PubMed: 8231890]
49. Krishnamurthy H, Weinbauer GF, Aslam H, Yeung CH, Nieschlag E. Quantification of apoptotic testicular germ cells in normal and methoxyacetic acid-treated mice as determined by flow cytometry. J Androl. 1998; 19:710–717. [PubMed: 9876022]
50. Nebel BR, Amarose AP, Hacket EM. Calendar of gametogenic development in the prepuberal male mouse. Science. 1961; 134:832–833. [PubMed: 13728067]
51. Suter L, Koch E, Bechter R, Bobadilla M. Three-parameter flow cytometric analysis of rat spermatogenesis. Cytometry. 1997; 27:161–168. [PubMed: 9012383]
52. Weil M, Jacobson MD, Raff MC. Are caspases involved in the death of cells with a transcriptionally inactive nucleus? Sperm and chicken erythrocytes. J Cell Sci. 1998; 111(Pt 18): 2707–2715. [PubMed: 9718364]
53. Meilhac O, Zhou M, Santanam N, Parthasarathy S. Lipid peroxides induce expression of catalase in cultured vascular cells. J Lipid Res. 2000; 41:1205–1213. [PubMed: 10946007]
54. Jow WW, Schlegel PN, Cichon Z, Phillips D, Goldstein M, Bardin CW. Identification and localization of copper-zinc superoxide dismutase gene expression in rat testicular development. J Androl. 1993; 14:439–447. [PubMed: 8294228]
55. Peltola V, Huhtaniemi I, Ahotupa M. Antioxidant enzyme activity in the maturing rat testis. J Androl. 1992; 13:450–455. [PubMed: 1429221]
56. Roveri A, Casasco A, Maiorino M, Dalan P, Calligaro A, Ursini F. Phospholipid hydroperoxide glutathione peroxidase of rat testis. Gonadotropin dependence and immunocytochemical identification. J Biol Chem. 1992; 267:6142–6146. [PubMed: 1556123]
57. van der Brug MP, Blackinton J, Chandran J, Hao LY, Lal A, Mazan-Mamczarz K, Martindale J, Xie C, Ahmad R, Thomas KJ, Beilina A, Gibbs JR, Ding J, Myers AJ, Zhan M, Cai H, Bonini NM, Gorospe M, Cookson MR. RNA binding activity of the recessive parkinsonism protein DJ-1 supports involvement in multiple cellular pathways. Proc Natl Acad Sci U S A. 2008; 105:10244–10249. [PubMed: 18626009]
58. Ufer C, Wang CC, Fahling M, Schiebel H, Thiele BJ, Billett EE, Kuhn H, Borchert A. Translational regulation of glutathione peroxidase 4 expression through guanine-rich sequence-

binding factor 1 is essential for embryonic brain development. Genes Dev. 2008; 22:1838–1850. [PubMed: 18593884]

59. Yao Y-G, Ellison FM, McCoy JP, Chen J, Young NS. Age-dependent accumulation of mtDNA mutations in murine hematopoietic stem cells is modulated by the nuclear genetic background. Human Molecular Genetics. 2007; 16:286–294. [PubMed: 17185390]
60. Yaman, Soygur T, Yilmaz E, Elgun S, Keskinege A, Gogus O. The significance of testicular reactive oxygen species on testicular histology in infertile patients. Int Urol Nephrol. 1999; 31:395–399. [PubMed: 10672960]
61. Koksal IT, Usta M, Orhan I, Abbasoglu S, Kadioglu A. Potential role of reactive oxygen species on testicular pathology associated with infertility. Asian J Androl. 2003; 5:95–99. [PubMed: 12778317]
62. Filho DW, Torres MA, Bordin ALB, Crezcynski-Pasa TB, Boveris A. Spermatic cord torsion, reactive oxygen and nitrogen species and ischemia-reperfusion injury. Molecular Aspects of Medicine. 2004; 25:199–210. [PubMed: 15051328]
63. Matzuk MM, Dionne L, Guo Q, Kumar TR, Lebovitz RM. Ovarian Function in Superoxide Dismutase 1 and 2 Knockout Mice. Endocrinology. 1998; 139:4008–4011. [PubMed: 9724058]
64. Li Y, Huang TT, Carlson EJ, Melov S, Ursell PC, Olson JL, Noble LJ, Yoshimura MP, Berger C, Chan PH, Wallace DC, Epstein CJ. Dilated cardiomyopathy and neonatal lethality in mutant mice lacking manganese superoxide dismutase. Nat Genet. 1995; 11:376–381. [PubMed: 7493016]
65. Lebovitz RM, Zhang H, Vogel H, Cartwright J Jr, Dionne L, Lu N, Huang S, Matzuk MM. Neurodegeneration, myocardial injury, and perinatal death in mitochondrial superoxide dismutase-deficient mice. Proc Natl Acad Sci U S A. 1996; 93:9782–9787. [PubMed: 8790408]
66. Aruldhas MM, Subramanian S, Sekar P, Vengatesh G, Chandrahasan G, Govindarajulu P, Akbarsha MA. Chronic chromium exposure-induced changes in testicular histoarchitecture are associated with oxidative stress: study in a non-human primate (Macaca radiata Geoffroy). Hum Reprod. 2005; 20:2801–2813. [PubMed: 15980013]
67. Mishra M, Acharya UR. Protective action of vitamins on the spermatogenesis in lead-treated Swiss mice. Journal of Trace Elements in Medicine and Biology. 2004; 18:173–178. [PubMed: 15646264]
68. Fisch H. Older men are having children, but the reality of a male biological clock makes this trend worrisome. Geriatrics. 2009; 64:14–17. [PubMed: 19256577]

Highlights

- Oxidative stress increases in old *Immp2l* mutant mice with impaired spermatogenesis.
- Apoptosis is increased in round spermatids, 2N cells, and spermatocytes.
- Testicular cytosolic GPX4 decreases in mutant mice with impaired spermatogenesis.
- Mitochondrial DNA mutation is not involved in impaired spermatogenesis of mutants.

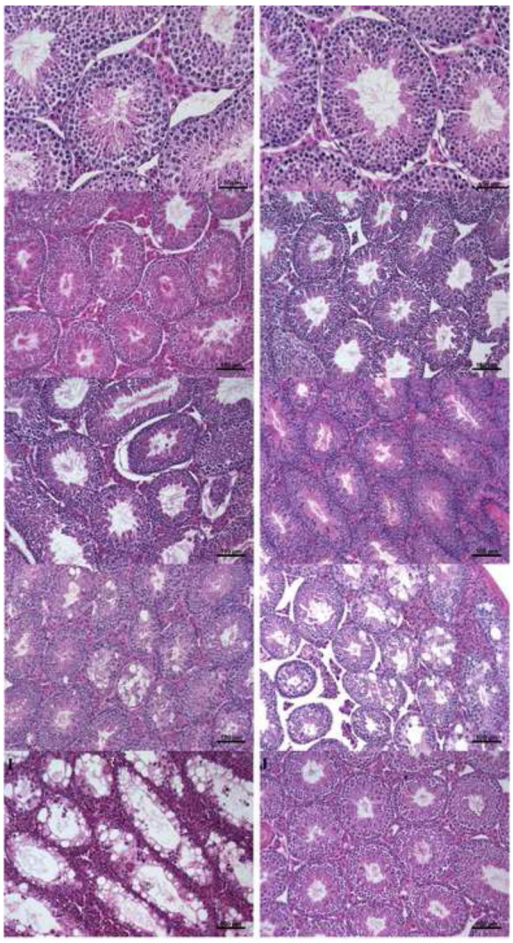

Fig. 1. Time course of age-dependent spermatogenic impairment in mutant males

(**A–B**). Spermatogenic development is normal in prepubertal mutant mice. In the testes of 35-day-old controls (A) and mutants (B), elongated spermatids in the seminiferous lumen were both observed. (**C–D**). Normal spermatogenesis in 7-month-old control (C) and mutant (D) mice. **E.** Qualitatively normal spermatogenesis in 9-month-old mutants. **F**. Qualitatively normal spermatogenesis in 10-month-old mutants. **G**. Some mutant mice of 10.5 months start to show degenerated seminiferous tubules. **H.** Impaired spermatogenesis in 11-month-old mutants. **I**. Impaired spermatogenesis in 15-month-old mutants. **J**. Normal spermatogenesis in 15-month-old control males. Scale bars in A–B: 50 μm; scale bars in C–J: 100 μm.

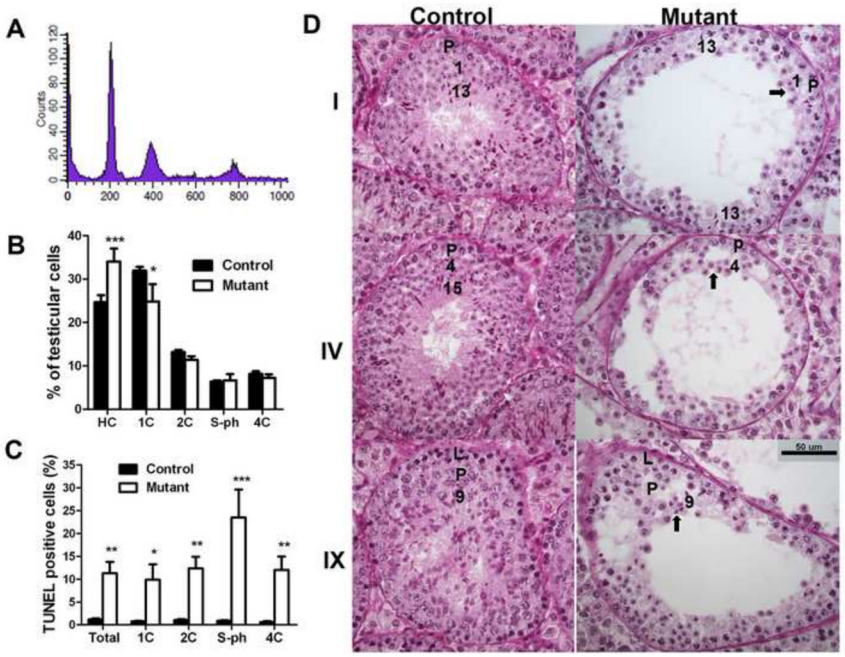

Fig. 2. Germ cell types affected in aged mutant mice

A. Representative diagram from flow cytometry analysis of PI stained testicular cells (13-month-old control mouse). **B**. Percentage of testicular cell populations between 13-month-old controls (n=5) and mutants (n=4). **C**. Percentage of apoptotic (TUNEL positive) cells in different testicular cell populations between 13-month-old controls (n=5) and mutants (n=4). PI (for DNA ploidy) and FITC (for TUNEL assay) double-channel flow cytometry was performed. **D**. PAS staining of testis sections from 11-month-old mice. Cross-sections of the same stages of germ cell association from controls and mutants are shown. Roman numerals indicate the stage of the association determined by acrosome morphology. Arabic numbers indicate the steps of the spermatids. The arrows point to the spermatids used for the determination of the stage of the association. L indicates leptotene spermatocytes and P indicates pachytene spermatocytes. Scale bar: 50 μm. Mean ± SEM are presented in **B** and **C**. *, ** and *** indicate $p<0.05$, $p<0.01$, and $p<0.001$, respectively, by two-way ANOVA and Bonferroni post-tests.

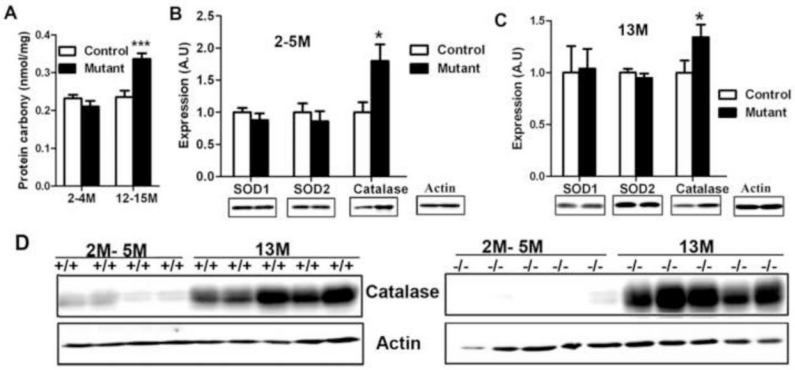

Fig. 3. Analysis of protein carbonyl content and antioxidant enzyme expression in testes of mutant mice

A. Protein carbonyl content is increased in 13-month-old mutant mice. Mean ± SEM of 5 mice for each group are presented. *** indicates $p<0.001$ by two-way ANOVA and Bonferroni post-tests. (**B, C**). Expression of antioxidant enzymes SOD1, SOD2, and catalase in testes of 2-~5-month-old mice (**B**) and 13-month-old mice (**C**). Mean ± SEM (n=5 for each group) of integrated density analyzed by Image J software are presented. Loading was normalized by β-actin. * indicates $p<0.05$ by t-tests. **D.** Catalase protein was increased in 13-month-old mice than in 2-~5-month-old mice.

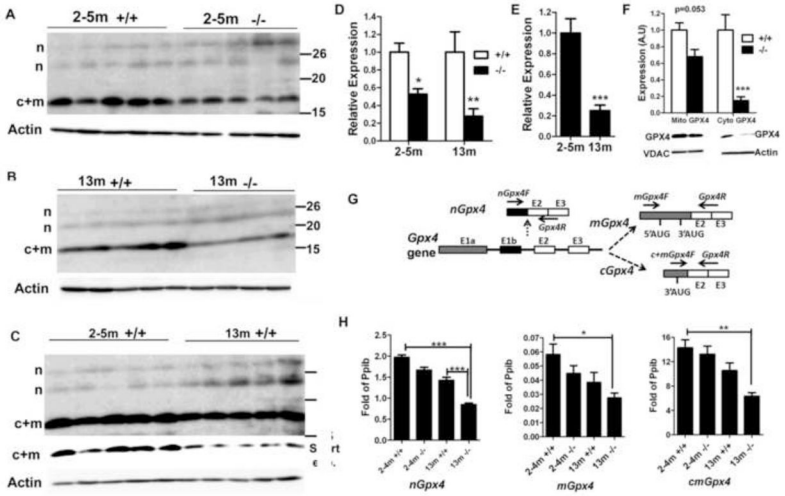

Fig. 4. Analysis of *Gpx4* expression at the protein and mRNA levels

A–C. Western blotting comparison of GPX4 expression between 2-~5-month-old control and mutant mice (**A**), 13-month-old control and mutant mice (**B**), and 2-~5-month-old and 13-month-old control mice (**C**). The expression of c+mGPX4 (c+m) was decreased in mutant mice relative to age-matched control mice, and in old mice relative to young mice. The expression of nGPX4 (n) did not differ among groups. In **C**, a longer exposure was used to show the relatively weak bands of nGPX4. The row with "short exp." indicates the result of short exposure time to avoid saturation. **D.** Densitometry analysis (integrated density by Image J software) of c+mGPX4 protein expression based on **A** and **B**. Mean ± SEM for each group is presented. The expression levels of control mice were set as 1. * and ** indicate $p<0.05$ and $p<0.01$, respectively by Bonferroni post-tests following two-way ANOVA. **E.** Densitometry analysis (integrated density by Image J software) of c+mGPX4 protein expression based on **C**. Mean ± SEM of 5 mice for each group is presented. The expression level of 2-~5-month-old mice was set as 1. *** indicates $p<0.001$ between 2-~5-month-old and 13-month-old control mice by t-test. **F**. Reduction of cGPX4 in 13-month-old mutant males. mGPX4 showed only a small reduction, but cGPX4 was significantly reduced in mutants versus controls. Mean ± SEM of 4 mice per group is shown. *** indicates $p<0.001$ by Bonferroni post-tests following two-way ANOVA. VDAC1 and β-actin were used for loading controls for mitochondrial and cytosolic protein, respectively. Expression of samples from control mice was set as 1. **G**. Location of primers used for detection of *nGpx4*, *mGpx4*, and *c+mGpx4*. Ten nucleotides from primer *Gpx4R* pair with exon 2 and 10 nucleotides pair with exon 3. **H.** Real-time RT-PCR comparison of *nGpx4*, *mGpx4*, and *c+mGpx4* levels among groups. Pooled cDNA from 5 mice/group was analyzed. Shown is the mean ± SEM of three independent real-time PCR assays. Expression is expressed as fold of internal control gene *Ppib*. *, ** and *** indicate $p<0.05$, $p<0.01$ and $p<0.001$, respectively, between indicated groups analyzed by Bonferroni post-tests following two-way ANOVA.

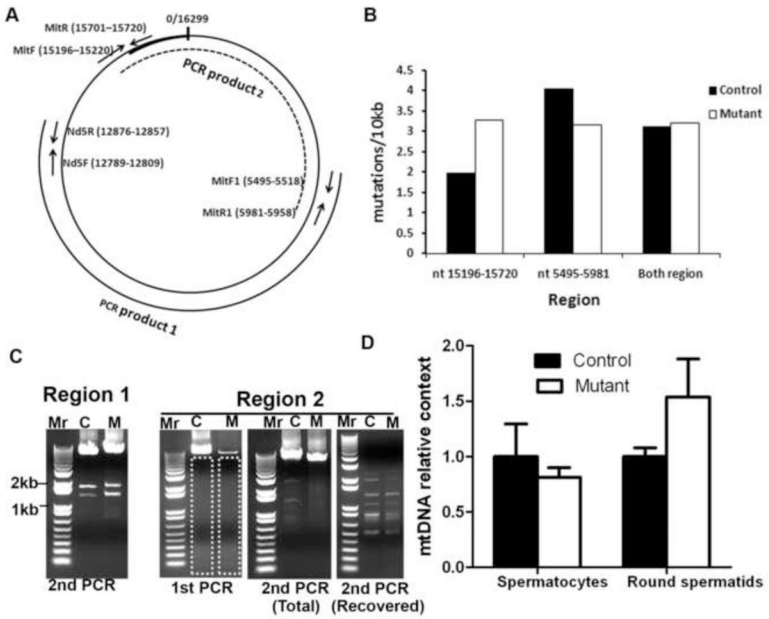

Fig. 5. Analysis of mtDNA mutation for germ cells from 11-month-old mice

A. Location of primers used for PCR amplification. MitF+MitR, MitF1+MitR1 were used to amplify mtDNA for subcloning and sequencing analysis. Nd5F+Nd5R were used in quantitative PCR to compare mtDNA content. The regions amplified (PCR product 1 and PCR product 2) in long-range PCR for deletion analysis are also shown. **B.** mtDNA mutation rates of elongated spermatids (mixed from 3 males of the same genotype) from 11-month control and mutant mice. **C.** Long-range PCR analysis of large mtDNA deletion. Nested PCR was used to detect possible large mtDNA deletion from elongated spermatid mtDNA. Dashed box indicates the gel recovered for DNA purification after the first round of PCR. “Second PCR (total)” indicates using the total PCR product from the first PCR as the template in the second PCR. “Second PCR (recovered)” indicates using the purified DNA from boxed gel as the template in the second PCR. **D.** mtDNA DNA content in spermatocytes and round spermatids of control and mutant mice. No significant differences were noted. mtDNA content in control mice was set as 1. Mean ± SEM of three control and three mutants are presented. Triplicate assays were performed on each sample.

Table 1

Spermatogenic damage observed at different ages

Age (mo)	+/+		−/−	
	With 30% impaired seminiferous tubules*	With 80% impaired seminiferous tubules*	With 30% impaired seminiferous tubules*	With 80% impaired seminiferous tubules*
7	0/2	0/2	0/4	0/4
10	0/1	0/1	0/2	0/2
10.5	0/1	0/1	1/3	0/3
11	N/A	N/A	3/3	2/3
12	0/4	0/4	4/4	0/4
13	0/5	0/5	5/5	0/5
14	0/3	0/3	8/8	1/8
15	0/3	0/3	3/3	1/3

* Number of animals with damages/total animals examined.